

## Magnetic Properties of V/Ag Multilayered Superconductors

Hiromasa MAZAKI,\* Kazushi KANODA,\* Nobuyoshi HOSOITO,\*\*  
and Teruya SHINJO\*\*

Received January 26, 1987

We have made measurements of the magnetic-field penetration depth  $\lambda$  of V/Ag proximity-coupled multilayers for the first time. The layer-thickness dependence of  $\lambda$  exhibits a nonmonotonic behavior, which is interpreted as a crossover from a single superconductor to a composite one. When the Ag layer becomes thicker, the temperature dependence of  $\lambda$  begins to deviate from that of usual superconductors, showing that the proximity effect is involved. In addition, from  $\lambda$  and our previously found upper-critical-field parameters, the Ginzburg-Landau parameter was obtained for the short-period multilayers.

**KEY WORDS:** Superconducting multilayer/ Proximity effect/ Field penetration/ Ginzburg-Landau parameter/

### I. INTRODUCTION

Recent developments in thin film technology have made possible to produce a variety of multilayers, arousing interest in novel properties unseen in conventional materials. As a typical case, many superconducting multilayers have been fabricated and investigated in a large number of experiments.<sup>1)</sup>

Concerning the thermodynamic properties, the variation of the transition temperature  $T_c$  has been studied for various multilayers.<sup>1)</sup> The specific heat has also been investigated in the Nb/Zr systems.<sup>2)</sup> As to the electromagnetic properties, the upper critical field  $H_{c2}$  has been most extensively studied, because  $H_{c2}$  can probe the superconducting dimensionality. Indeed, dimensional crossover and related phenomena have been neatly observed with Nb/Ge,<sup>3)</sup> Nb/Cu,<sup>4)</sup> V/Ag,<sup>5)</sup> V/Ni,<sup>6)</sup> and V/Fe<sup>7)</sup> multilayers. However, to the authors' knowledge, the magnetic-field penetration depth, which is one of the fundamental electromagnetic quantities, has not yet been uncovered for multilayered systems.

We have made for the first time measurements of the magnetic-field penetration depth  $\lambda$  of V/Ag proximity-coupled multilayers. The films were prepared by ultrahigh-vacuum electron-beam evaporation. Total thicknesses range 3100–6400 Å. Since field penetration is sensitive to the surface state, both sides of each sample end with Ag layers, which are stable in air and have a lustrous surface. The artificial periodicity was examined by X-ray diffraction, and the difference between the designed and the observed periods was found to be less than 5%. The superconducting transition measured by the inductive change in a field perpendicular to the

\* 間崎啓匡, 鹿野田一司: Laboratory of Nuclear Radiation, Institute for Chemical Research, Kyoto University, Kyoto 606.

\*\* 細糸信好, 新庄輝也: Laboratory of Solid State Chemistry, Institute for Chemical Research, Kyoto University, Uji 611.

films gives  $\Delta T < 20$  mK for the 10–90% width. Details of the sample preparation as well as the structural quality were previously reported.<sup>8)</sup> A brief account of the  $\lambda$  results was also given earlier.<sup>9)</sup> In addition, the Ginzburg-Landau parameter, which is one of the fundamental magnetic parameters, is also discussed.

## II. MEASUREMENTS

The parameters of the multilayers studied here are listed in Table I. The penetration depth was determined by means of the ac susceptibility ( $\chi_{||} = \chi'_{||} - i\chi''_{||}$ ) with the field parallel to the films. In this geometry, field penetration takes place

Table I. Sample parameters of V/Ag multilayers.

$d_V/d_{Ag}$ (Å/Å)	$D$ (Å)	$T_c^z$ (K)	$\rho$ ( $\mu\Omega\text{cm}$ )
30/15	1985	2.31	20.9 (31.7) <sup>b</sup>
40/20	1980	2.86	18.7 (26.5) <sup>b</sup>
100/50	3150	3.64	12.8 (14.2) <sup>b</sup>
100/100	3100	3.33	8.37
100/200	4700	2.44	4.15
160/320	5120	2.86	3.01
200/400	6400	3.34	2.36
240/480	5520	3.38	2.03

<sup>a</sup>Transition temperatures are determined from measurements of  $\chi_{||}$ , and are slightly different from those from the resistive transition.

<sup>b</sup>For multilayers with the Ag-layer thickness less than 100 Å, covering Ag layers are 100-Å thick. The values in parentheses are obtained after subtraction of the contribution of the covering layers.

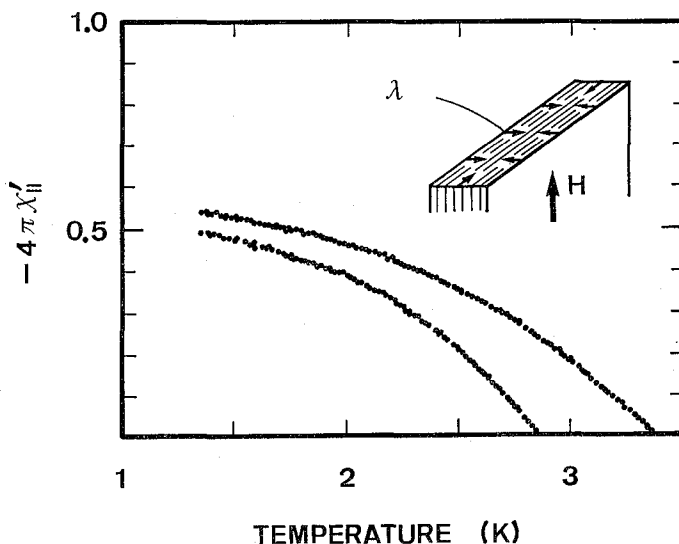


Fig. 1. Typical results of the magnetic susceptibility (real part) vs temperature. Inset shows the sample geometry against applied field.  $\lambda$  is the penetration depth perpendicular to the layers.

both from the Ag surfaces in the direction perpendicular to the layers and from the film edges in the parallel direction (see Inset of Fig. 1). Considering the sample dimension, the former penetration is principally responsible for  $\chi_{||}$ . Hence the penetration depth  $\lambda$  derived from  $\chi_{||}$  is in the perpendicular direction.

The measurements of ac susceptibility were performed with a Hartshorn-type mutual inductance bridge.<sup>10)</sup> Two or four sheets of samples ( $8 \times 20 \text{ mm}^2$ ) are mounted in the cryostat coil. They were placed directly into liquid He, because  $T_c < 4.2 \text{ K}$  for all samples. Null adjust and phase settings are made above  $T_c$ . The off-balance signal is detected by a two-phase lock-in analyzer as a function of temperature. The change in mutual inductance resulting from the superconductive diamagnetism of the films is very small (typically of the order of  $0.1 \mu\text{H}$ ). Therefore, when the temperature is lowered down to  $1.3 \text{ K}$  (the lowest temperature available), the contribution of the surroundings (including coils) to  $\chi_{||}$  becomes crucial. However, since no discernible phase shift was found in the bridge throughout the experimental temperature range, we can extract  $\chi_{||}$  of samples by subtracting the background from the raw data. The subtraction is made respectively for the in-phase and out-of-phase components. The absolute values of the real ( $\chi'_{||}$ ) and imaginary ( $\chi''_{||}$ ) parts are deduced with reference to the complete diamagnetism of Sn films having the thicknesses far greater than its penetration depth.

The measurements were carried out using 1-Oe 132-Hz ac field. We confirmed that no appreciable difference appeared by changing the applied field from 0.2 to 2 Oe and up to 500 Hz. For all samples,  $\chi''_{||}$  is nearly zero at all experimental temperatures, and henceforth we focus our discussion only on  $\chi'_{||}$ . Figure 1 shows typical results of  $\chi'_{||}$ , where  $-4\pi\chi'_{||}$  grows gradually as the temperature is lowered. Since the total thickness  $D$  of multilayer is comparable to  $\lambda$ , it is well reflected on the susceptibility. Assuming the field penetration to be exponential on a macroscopic scale, the magnetic induction in a multilayer is given by  $B_0 \cosh(z/\lambda)/\cosh(D/2\lambda)$ , where  $B_0$  is the applied induction and  $z=0$  denotes the center of the multilayer. Thus the relation between  $\lambda$  and  $\chi'_{||}$  is given as

$$-4\pi\chi'_{||} = 1 - \frac{2\lambda}{D} \tanh(D/2\lambda). \quad (1)$$

Note that in the measurement of  $\lambda$  for a *thin* film with a thickness comparable or smaller than  $\lambda$ , one must be careful to include the effect of film thickness. In such a system, if the electron mean free path is restricted by the film thickness, the field penetration is no longer exponential, and  $\lambda$  is not a specific value but depends on thickness.<sup>11)</sup> In our samples, however, the mean free path is much less than  $D$  (see below). Therefore the calculated  $\lambda$  represents the intrinsic value of the present V/Ag system, regardless of its total thickness.

### III. TRANSPORT PROPERTIES

In discussing the electromagnetic properties, we need to know the transport properties of the system under consideration. For this purpose, we measured the

resistivity parallel to the layers  $\rho$ , where the films deposited on mylar sheets were cut into a strip ( $1 \times 10 \text{ mm}^2$ ) and directly immersed in the liquid-He bath. The measurements were made with the four-probe method, where silver paint was used for electric contact.

$\rho$  just above  $T_c$  is shown in Fig. 2 as a function of Ag-layer thickness  $d_{Ag}$ .<sup>12)</sup> Numerical values of  $\rho$  are given in Table I. As seen in the figure,  $\rho$  decreases with increasing  $d_{Ag}$ . Referring to the change in  $\rho$  of the samples with the same thickness ratio  $d_V:d_{Ag}$ , we find that scattering at the V/Ag interface restricts substantially the mean free path of electrons in the multilayers. However, if the boundary scattering is the only contribution to the resistivity, the slope of  $\rho$  vs  $d_{Ag}$  (or  $d_V$ ) should be  $-1$ . Deviation of the experimental points from the slope of  $-1$  for the small period suggests that at least one of the intrinsic mean free path within the V and Ag layers is comparable or smaller than the layer thickness.

In order to determine practical values of the mean free paths  $l_V$  and  $l_{Ag}$  in the multilayers, we assume that  $\rho$  is given as a parallel junction of  $\rho_V$  and  $\rho_{Ag}$  (the resistivities of the V and Ag layers, respectively). Thus  $\rho$  is expressed as

$$\frac{1}{\rho} = \frac{d_V}{d_V + d_{Ag}} \cdot \frac{1}{\rho_V} + \frac{d_{Ag}}{d_V + d_{Ag}} \cdot \frac{1}{\rho_{Ag}}. \quad (2)$$

As the first step, we attempted to evaluate  $\rho_V$  in the thick limit with otherwise prepared single V films. The observed resistivities scatter considerably ( $20\text{--}35 \mu\Omega\text{cm}$ ), probably due to surface oxidization. However, it is not unreasonable to suppose that  $\rho_V$  is  $20 \mu\Omega\text{cm}$  at most, which corresponds to  $l_V \approx 20 \text{ \AA}$ .<sup>13)</sup> On this supposition, we may say that for four samples denoted by solid circles in Fig. 2 ( $d_V \geq 100$

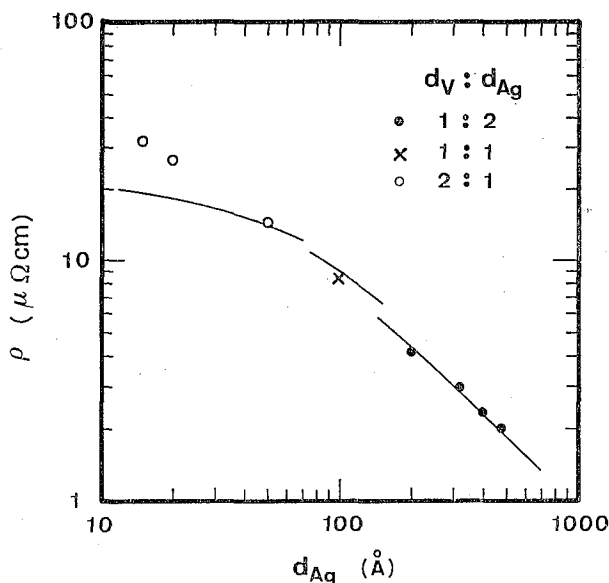


Fig. 2. Normal-state resistivity as a function of Ag-layer thickness. Solid curves are calculated on the assumption of the bulk resistivity in the V layers ( $15 \mu\Omega\text{cm}$ ) and the thickness-dependent resistivity in the Ag layers.

Å), the contribution of boundary scattering in the V layers is so small that  $\rho_V$  in Eq. (2) becomes constant. Hence the variation in  $\rho$  with the slope of nearly  $-1$  is surely attributed to the boundary scattering of electrons in the Ag layers.

As is well known, Ag can be approximated as a free electron system. In accordance with the Drude model,  $\rho_{Ag}$  is related to the mean free path  $l_{Ag}$  in the Ag layers by  $\rho_{Ag}=840/l_{Ag}$ ,<sup>14)</sup> where  $\rho_{Ag}$  is in unit of  $\mu\Omega\text{cm}$  and  $l_{Ag}$  is in Å. Assuming the proportionality of  $l_{Ag}$  to the thickness  $d_{Ag}$ , we put  $l_{Ag}=\alpha d_{Ag}$ , where  $\alpha$  is a constant. Thus we get  $\rho_{Ag}=840/\alpha d_{Ag}$ . Since the second term in Eq. (2) is dominant for above four samples, we can determine  $\alpha$  by fitting the second term to the experimental results (solid circles) in Fig. 2, from which we get  $\alpha=1.3$ , i.e.,  $l_{Ag}=1.3d_{Ag}$ . This relation is of course assumed applicable for all other experimental points in Fig. 2.

Once  $\rho_{Ag}$  is thus determined, substituting this value and the experimental values of  $\rho$  into Eq. (2), we can calculate  $\rho_V$  for other samples with smaller  $d_{Ag}$ , where the first term is comparable to the second term. Referring to the theoretical result of  $l_V$  vs  $\rho_V$ ,<sup>13)</sup> we find  $l_V$  vs  $d_V$  (see Fig. 3), where  $l_V$  decreases with decreasing  $d_V$ , reflecting the effect of the V/Ag boundary scattering of electrons in thin V layers. In the mean time, for V(100 Å)/Ag(50 Å) we get  $\rho_V=15 \mu\Omega\text{cm}$ , which corresponds to  $l_V \simeq 22$  Å. One can say that this value is almost the bulk value of this V, because  $l_V$  is several times smaller than  $d_V$  ( $=100$  Å).

To see how the effect of boundary scattering in the V layers appears in  $\rho$ , we in turn substitute the bulk value  $\rho_V=15 \mu\Omega\text{cm}$  into Eq. (2). The values of  $\rho$  thus calculated are given by solid curves in Fig. 2. Deviations of far left two experimental points from the curve unambiguously indicate that in this region  $l_V$  is affected by the V-layer thickness.

Finally, we note that the V and Ag layers are dirty in a sense of superconductivity. The dirty nature of the V layers is evident from the short mean free path ( $l_V \lesssim 22$  Å). As to the Ag layers, the coherence length  $\xi_{Ag}$  must be compared with the mean free path  $l_{Ag}$ , where  $\xi_{Ag}(T) = (\hbar v_{Ag} l_{Ag} / 6\pi k_B T)^{1/2}$ ,  $v_{Ag}$  is the Fermi velocity in Ag.<sup>15)</sup> Adopting the relation  $l_{Ag} = 1.3d_{Ag}$ , we estimate  $\xi_{Ag}(T)$ , of which the values at  $T_c$  as well as  $l_{Ag}$  are tabulated in Table II. Evidently  $\xi_{Ag}(T_c) > l_{Ag}$  for all samples,

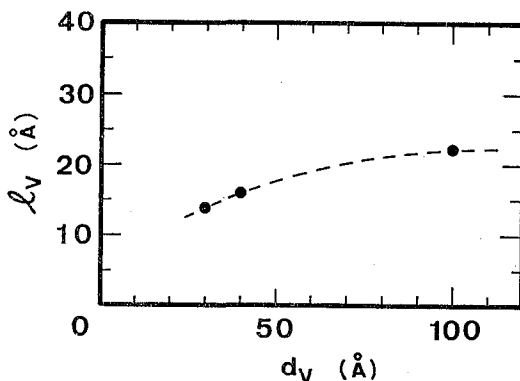


Fig. 3. Electron mean free path in the V layers as a function of layer thickness.

Table II. Electron mean free paths and coherence lengths in the Ag layers.

$d_V/d_{Ag}$ (Å/Å)	$l_{Ag}$ (Å)	$\xi_{Ag}(T_c)$ (Å)
30/15	20	215
40/20	26	225
100/50	65	314
100/100	130	461
100/200	260	742
160/320	416	903
200/400	520	918
240/480	624	1020

although  $\xi_{Ag}(T_c)$  approaches  $l_{Ag}$  in thicker Ag layers. Since  $\xi_{Ag}(T)$  increases with decreasing temperature, the above inequality holds down to 0 K. Therefore we conclude that the Ag layers may also be treated in the dirty limit.

#### IV. LAYER-THICKNESS DEPENDENCE OF $\lambda$

Based on the above specific transport properties in the V and Ag layers, we first compare the penetration depth for multilayers of the same thickness ratio ( $d_V: d_{Ag}=2:1$ ). Figure 4 shows  $\lambda$  at several reduced temperatures as a function of multilayer period  $d$  ( $=d_V+d_{Ag}$ ). At all temperatures  $t$ ,  $\lambda$  increases sharply with the decrease of  $d$ , and even seems to diverge at  $d \sim 0$ .

This result is qualitatively understood by considering the fact that the system becomes dirtier for smaller  $d$ . Since there exists no theoretical treatment of  $\lambda$  for multilayered systems, we discuss the above feature in the framework of the conventional theory for homogeneous superconductors.

The penetration depth in the dirty local limit  $\lambda^d(T)$  is given as<sup>11)</sup>

$$\lambda^d(T) = \lambda_L(T) J(0, T)^{-1/2} (\xi_0/l)^{1/2}, \quad (3)$$

where  $\lambda_L(T)$  is the London penetration depth,  $\xi_0$  is the BCS coherence length,  $l$  is the mean free path, and  $J(R, T)$  is the integral kernel defined by BCS.<sup>16)</sup> Using the basic formulae<sup>17)</sup> for  $\lambda_L(0)$ ,  $\xi_0$ , and  $l$ , Eq. (3) reduces to

$$\lambda^d(T) = 1.05 \times 10^{-2} J^{-1/2}(0, T) \frac{\lambda_L(T)}{\lambda_L(0)} \left( \frac{\rho}{T_c} \right)^{1/2} \text{ cm}, \quad (4)$$

where  $\rho$  is in unit of  $\Omega\text{cm}$ . Since any normal metal with a finite mean free path falls into the dirty limit category at 0 K, the dirty limit treatments are more realistic at low temperature, at least for the Ag layers. Thus substituting  $T=0$  into Eq. (4), one gets

$$\lambda^d(0) = 1.05 \times 10^{-2} (\rho/T_c)^{1/2} \text{ cm}, \quad (5)$$

where  $J(0, 0)=1$ . Equation (5) includes only experimentally determined quantities so that the penetration depth can be discussed without any fitting parameters.  $\lambda^d(0)$

is evaluated using only the experimental values of  $\rho^{18)}$  and  $T_c$  (tabulated in Table I), as shown in Fig. 4.  $\lambda^d(0)$  reproduces well the expected  $\lambda$  at  $t=0$ , and in particular its  $d$ -dependence is in good agreement with the observed  $\lambda$ . This means that the samples with smaller  $d$  behave like a homogeneous superconductor, i.e., the field penetration is mostly determined by  $T_c$  and the mean free path obtained from  $\rho$ .

The above nature like a single superconductor was examined by changing  $d_{Ag}$  ( $d_V$  is fixed at 100 Å). In general, the penetration depth of a normal metal in contact with a superconductor is longer than that of the isolated superconductor. Therefore, if the multilayer is considered to be a composite material,  $\lambda$  should increase with increasing  $d_{Ag}$ . Figure 5 shows  $\lambda$  at several  $t$  for samples with the same  $d_V$  ( $=100$  Å) and different  $d_{Ag}$ . Contrary to the expectation, our observations showed

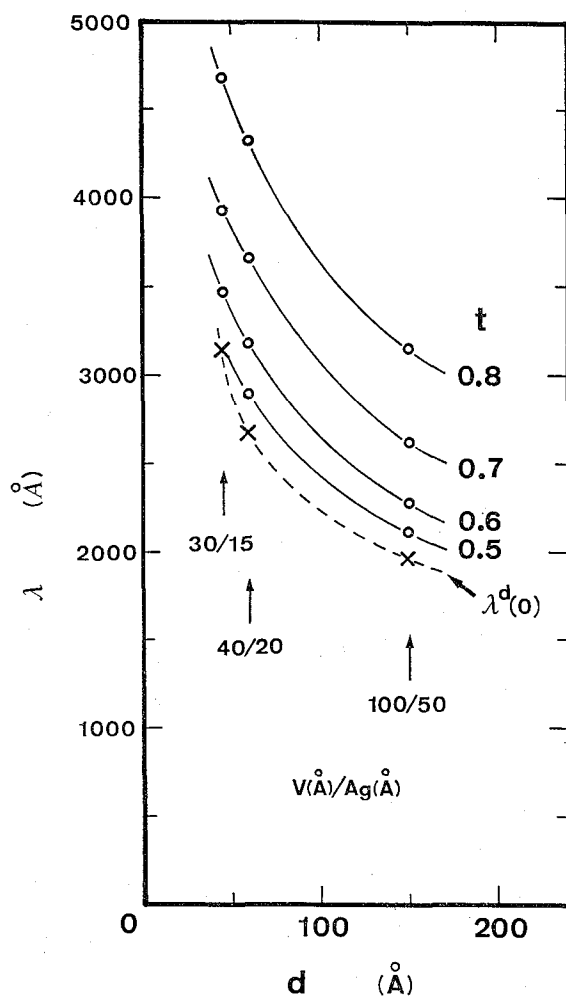


Fig. 4. Penetration depth vs multilayer period for samples with the same thickness ratio at several reduced temperatures  $t$ .  $\lambda^d(0)$  is the calculated values for a homogeneous superconductor in the dirty limit at  $t=0$ . Solid and dashed curves are guides for the eye unless otherwise denoted.

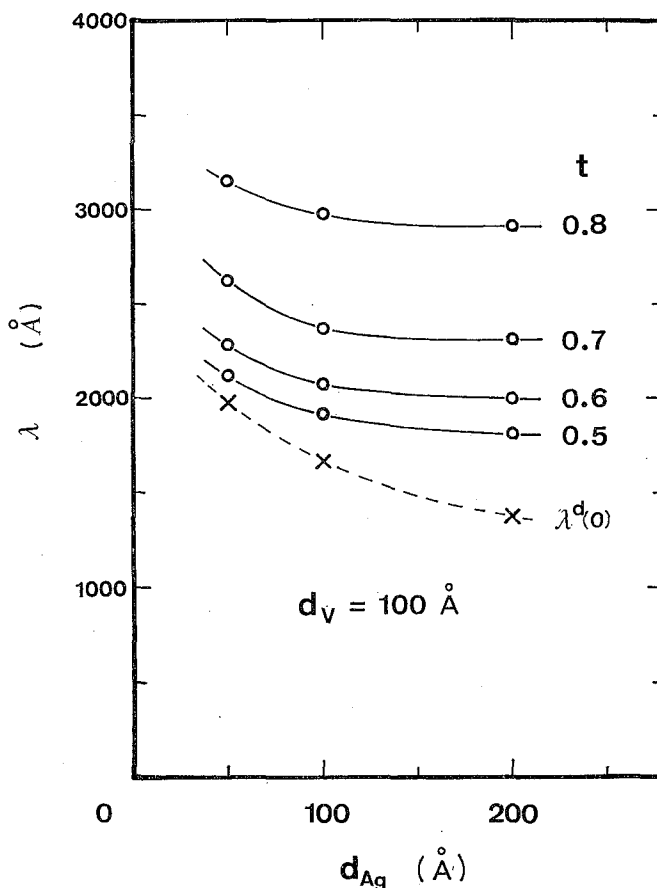


Fig. 5. Penetration depth vs Ag-layer thickness for samples with the same thickness of V layers at several reduced temperatures  $t$ . For  $\lambda^d(0)$ , see Fig. 4.

that  $\lambda$  decreases with increasing  $d_{Ag}$ , being similar to the  $d_{Ag}$ -dependence of  $\lambda^d(0)$  for a homogeneous superconductor.

For the samples with longer  $d$ , the behavior of  $\lambda$  becomes unusual. Figure 6 shows  $\lambda$  vs  $d$  at several  $t$  for samples with the same thickness ratio ( $d_V : d_{Ag} = 1:2$ ). As  $d$  increases  $\lambda$  first decreases like thinner samples. However, when  $d$  exceeds  $\sim 600$  Å,  $\lambda$  starts to grow. This peculiar feature is seen at all measured  $t$ . Note that the surface Ag layers are not responsible for this peculiarity, because a similar behavior of  $\lambda$  vs  $d$  holds even up to the high reduced temperature, where  $\lambda$  is far greater than  $d_{Ag}$ . The calculated  $\lambda^d(0)$  is also shown in the figure.  $\lambda^d(0)$  decreases monotonically with increasing  $d$ , and begins to deviate from the experimental  $\lambda$  at  $d \sim 600$  Å. This deviation can be interpreted as a kind of crossover from a single superconductor to a composite one. In other words, for the penetration depth, the coupling between the V layers weakens above the turnover thickness.

A comparison with our previously studied upper critical field parallel to the layers  $H_{c2||}(t)$  for the same samples<sup>5)</sup> may give some insight to this particular behavior

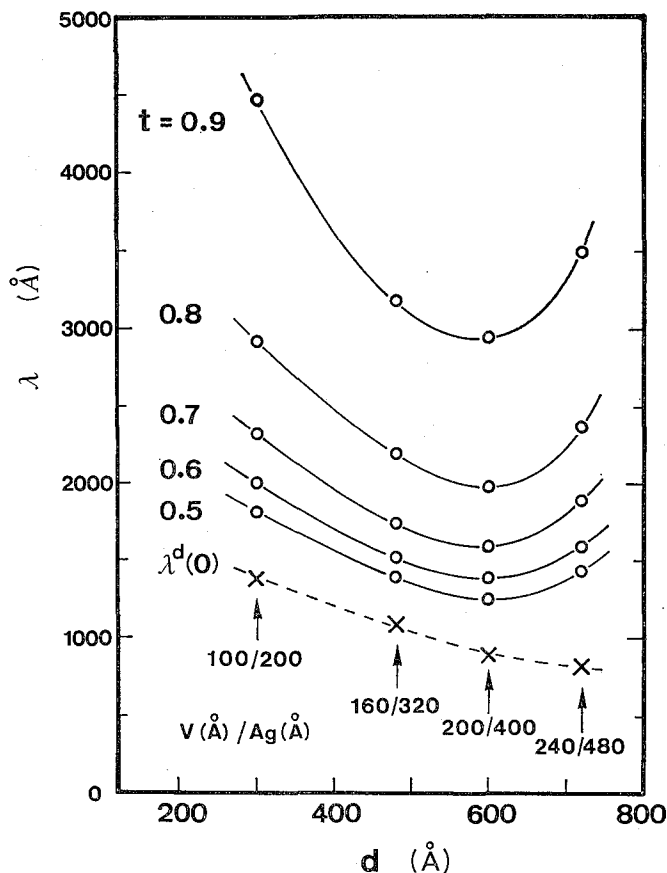


Fig. 6. Penetration depth vs multilayer period for samples with the same thickness ratio at several reduced temperatures  $t$ . For  $\lambda^d(0)$ , see Fig. 4.

of  $\lambda$ . When  $d$  is small enough,  $H_{c21}(t)$  behaves like a single, three-dimensional superconductor. But when  $d$  exceeds a certain threshold,  $H_{c21}(t)$  exhibits dimensional crossover and its onset shifts to higher  $t$  for greater  $d$ . This implies that the superconducting coupling between the V layers becomes weaker for greater  $d$ .

A weaker coupling should result in a longer penetration depth, so that  $\lambda$  is expected to increase with  $d$ , explaining the upward turn above  $d \sim 600$  Å. We emphasize here that the manner in which a composite nature appears on  $\lambda$  is qualitatively different from the case of  $H_{c21}$ . Even for a system which exhibits dimensional crossover in a *high field*, at *zero field* superconductivity extends all over the sample at all temperatures. Consequently, the multilayers always behave as three-dimensional from the point of view of the weak-field penetration depth. This is the reason why  $\lambda$  does not exhibit the drastic temperature dependence like  $H_{c21}$ . Instead, the composite nature moderately appears on the curve of  $\lambda$  vs  $d$ .

#### V. TEMPERATURE DEPENDENCE OF $\lambda$

Three typical results are presented: V(100 Å)/Ag(50 Å), V(160 Å)/Ag(320 Å),

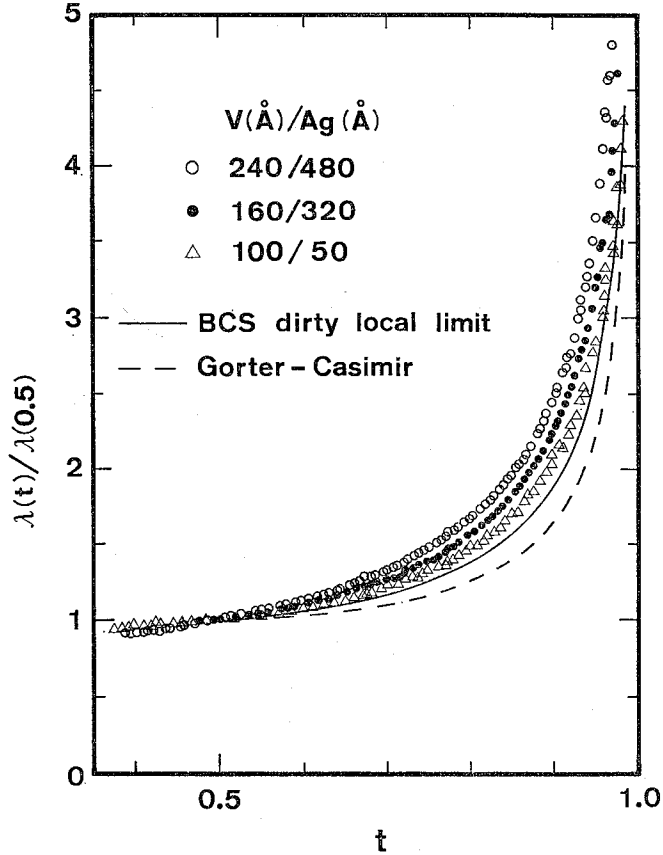


Fig. 7. Normalized penetration depth vs reduced temperature for three typical multilayers. Normalization is made at  $t=0.5$ .

and  $V(240 \text{ \AA})/Ag(480 \text{ \AA})$  as the multilayers with thin, intermediate, and thick Ag layers. Figure 7 shows  $\lambda$  as a function of reduced temperature for these samples, where  $\lambda$  is normalized at  $t=0.5$ . When the layer thickness increases, the variation of  $\lambda$  against  $t$  becomes more moderate. As demonstrated in Fig. 8, the difference is more visible in the plots of  $[\lambda(0.5)/\lambda(t)]^2$  vs  $t$ . For  $V(100 \text{ \AA})/Ag(50 \text{ \AA})$ , the temperature dependence seems to be linear near  $t=1$  and tends to saturate at lower temperature. In contrast,  $V(240 \text{ \AA})/Ag(480 \text{ \AA})$  exhibits an upward curvature in the temperature region above  $t \sim 0.7$  and increases almost linearly as the temperature is lowered further.  $V(160 \text{ \AA})/Ag(320 \text{ \AA})$  is located between them.

For reference, two curves for a homogeneous superconductor are also shown in the figures. One represents the empirical Gorter-Casimir law,  $\lambda \propto (1-t^4)^{-1/2}$ . It is well known that this curve reproduces the behavior of clean, Pippard-limit superconductors. As mentioned before, however, our system belongs to the dirty local regime. Therefore the large deviation of our results from this law is not surprising. The other is in the dirty local limit which is given as

$$\lambda \propto \left[ A(t) \tanh \frac{A(t)}{2k_B T} \right]^{-1/2}, \quad (6)$$

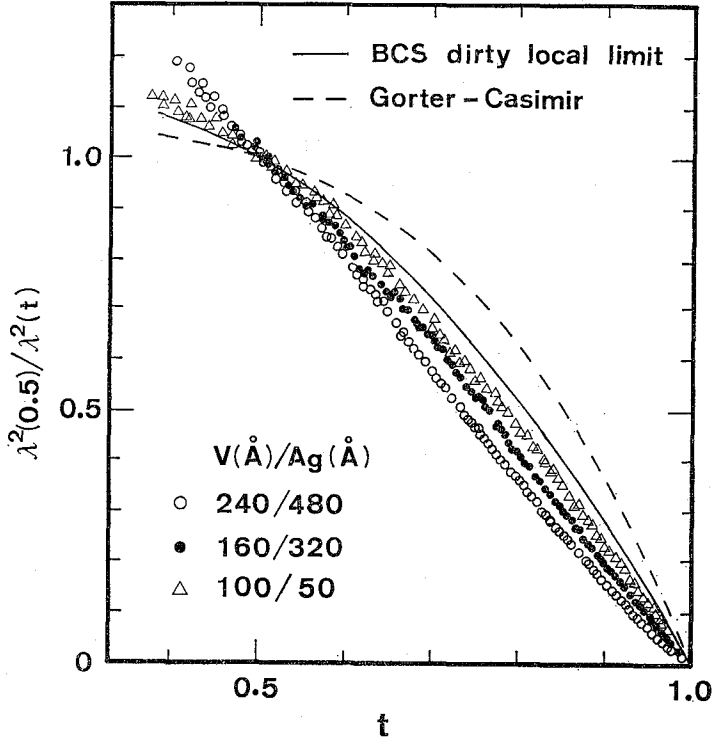


Fig. 8. Plots of  $[\lambda(0.5)/\lambda(t)]^2$  vs reduced temperature for the same samples in Fig. 7.

where  $\Delta(t)$  is the gap parameter. Although this relation could be realistic for our systems, the results exhibit remarkable differences, in particular when the layers become thicker.

We notice that the present results cannot be reproduced by any other limiting curve for a homogeneous superconductor. In the clean local limit  $\lambda$  is equal to the London penetration depth whose temperature dependence does not differ remarkably from the dirty local limit in the temperature region concerned. If the system goes to the nonlocal regime, the curve would approach the Gorter-Casimir's.<sup>11)</sup> Taking account of these facts, we should insist that the observed temperature dependence reveals a peculiar character of multilayers and should be attributed to the proximity effect.

The temperature dependence of field penetration into a normal-metal film (several thousand Å thick or more) superimposed on a thick superconductor has been investigated both theoretically and experimentally.<sup>19-24)</sup> According to these, the penetration differs from that of usual superconductors. When the temperature is lowered, it decreases more moderately, and continues to decrease even in the region where  $\lambda$  of the usual superconductors saturates. This behavior is mainly attributed to the temperature-dependent profile of the pair field amplitude in the normal metal. Hence the specific nature is expected to become more evident in thicker normal-metal films.

Turning attention to our systems, the present feature in  $\lambda(t)$  is qualitatively understood in the above context. Due to thin Ag layers,  $\lambda(t)$  for V(100 Å)/Ag(50 Å) bears a resemblance to the curve of usual superconductors in the dirty local limit. However, for the multilayers with thicker Ag layers, the proximity effect is reflected progressively on  $\lambda(t)$ . Indeed, for the latter  $[\lambda(0.5)/\lambda(t)]^2$  vs  $t$  changes from convex to concave at higher temperatures and does not saturate even at lower temperatures, being far different from usual superconductors. The above consideration although qualitative is consistent with the layer-thickness dependence of  $\lambda$ . For quantitative understandings, a refined theoretical treatment is needed.<sup>25)</sup>

## VI. GINZBURG-LANDAU PARAMETER

We first determine the Ginzburg-Landau (GL) penetration depth  $\lambda_{GL}(0)$ . In the GL theory, the penetration depth near  $T_c$  is given as

$$\lambda_{GL} = \lambda_{GL}(0)(1-t)^{-1/2}. \quad (7)$$

$\lambda_{GL}(0)$  can be obtained directly from the measured susceptibility: Near  $T_c$ ,  $\lambda$  should be much greater than  $D$ , so that Eq. (1) reduces to

$$-4\pi\chi'_{\parallel} = (1/12)(D/\lambda)^2. \quad (8)$$

Substituting Eq. (7) into Eq. (8) and differentiating with respect to  $t$ , we get

$$\lambda_{GL}(0) = D \left\{ 12 \left[ \frac{d}{dt} (4\pi\chi'_{\parallel}) \right]_{t=1} \right\}^{-1/2}. \quad (9)$$

Using the observed slope  $4\pi(d\chi'_{\parallel}/dt)_{t=1}$  in Eq. (9),  $\lambda_{GL}(0)$  is determined, of which the numerical values are tabulated in Table III. Figure 9 shows  $\lambda_{GL}(0)$  as a function of  $d$  or  $d_{Ag}$ . For reference, also shown is the dirty-limit value calculated from

$$\lambda_{GL}^d(0) = 6.45 \times 10^{-3} (\rho/T_c)^{1/2} \text{ cm}. \quad (10)$$

$\lambda_{GL}(0)$  tends to be in reasonable agreement with  $\lambda_{GL}^d(0)$  when the layer thickness becomes thinner, while deviation increases for thick-layer samples (Recall that the mean free path becomes progressively longer with increasing layer thickness).

The geometrical relation between the penetration depth and the coherence length in the anisotropic GL theory is depicted in Fig. 10. Anisotropic GL parameters  $\kappa_{\perp}$  and  $\kappa_{\parallel}$  are given as

Table III. Material parameters of V/Ag multilayers.

$d_V/d_{Ag}$ (Å/Å)	$\frac{d}{dt}(4\pi\chi'_{\parallel})_{t=1}$	$\lambda_{GL}(0)$ (Å)	$\xi_{GL\parallel}(0)$ (Å)	$\xi_{GL\perp}(0)$ (Å)	$\kappa_{\perp}$	$\kappa_{\parallel}$
30/15	0.0705	2160	113	92.4	19.2	23.4
40/20	0.0810	2010	112	91.9	17.9	21.9
100/50	0.375	1490	117	103	12.7	14.4
100/100	0.412	1390	153	132	9.14	10.6
100/200	0.900	1430	254	199	5.62	7.19

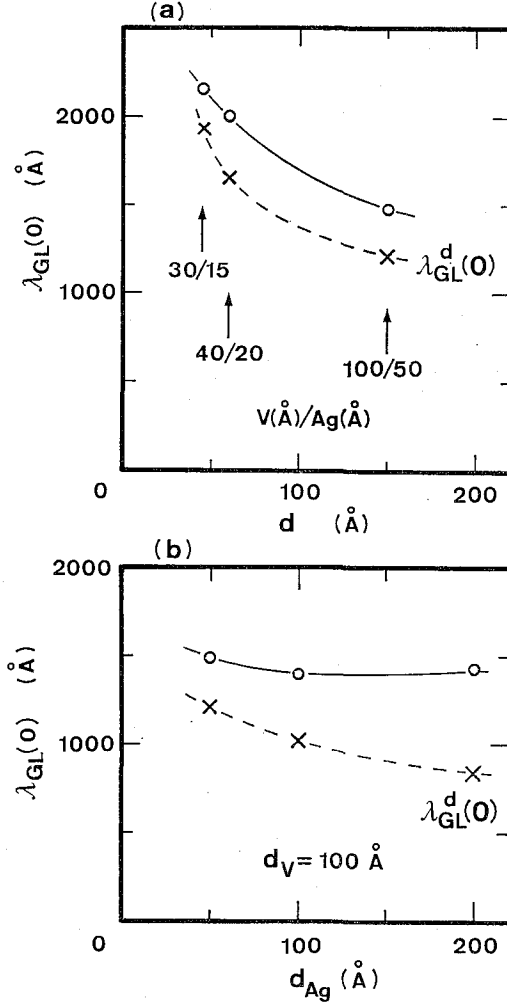


Fig. 9. Zero-temperature Ginzburg-Landau penetration depth vs multilayer period (a) or Ag-layer thickness (b).  $\lambda_{GL}^d(0)$  is the calculated values for a homogeneous superconductor in the dirty limit.

$$\kappa_{\perp} = \lambda_{GL}(0) / \xi_{GL\parallel}(0), \quad (11)$$

$$\kappa_{\parallel} = \lambda_{GL}(0) / \xi_{GL\perp}(0) = \lambda_{GL}(0) / \varepsilon \xi_{GL\parallel}(0), \quad (12)$$

where  $\xi_{GL\perp}(0)$  and  $\xi_{GL\parallel}(0)$  are the zero-temperature coherence lengths perpendicular and parallel to the layers. They were determined with the previous upper-critical-field measurements. The numerical values are listed in Table III.  $\varepsilon$  denotes the anisotropy parameter. Using the values of  $\xi_{GL\perp}(0)$ ,  $\xi_{GL\parallel}(0)$ , and  $\lambda_{GL}(0)$ , we evaluate  $\kappa_{\perp}$  and  $\kappa_{\parallel}$ , which are also listed in Table III. Figure 11a shows  $\kappa$  for samples of the same layer-thickness ratio ( $d_V : d_{Ag} = 2:1$ ). Both  $\kappa_{\perp}$  and  $\kappa_{\parallel}$  decrease with increasing  $d$ . The variation should be attributed to  $\lambda_{GL}(0)$  because  $\xi_{GL\parallel}(0)$  for these three samples is insensitive to  $d$  (see Table III). In Fig. 11b is shown  $\kappa$  vs  $d_{Ag}$  for multilayers with the same  $d_V$  ( $=100 \text{\AA}$ ), where both  $\kappa_{\perp}$  and  $\kappa_{\parallel}$  decrease further with the increase of

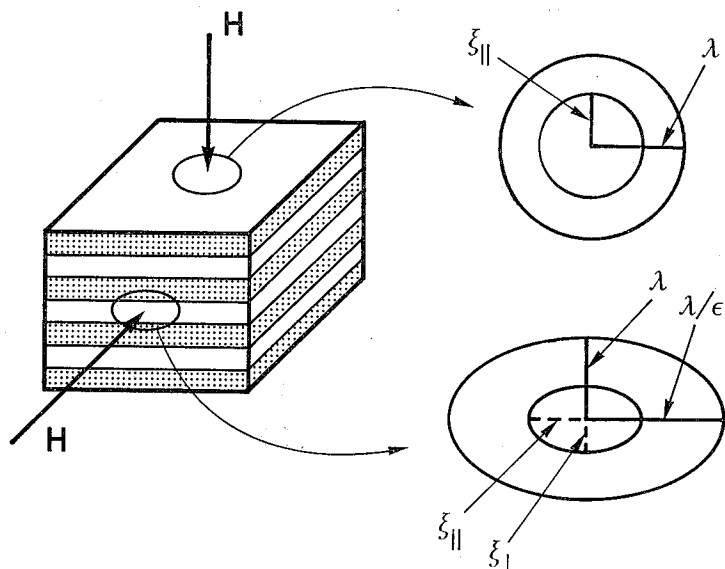


Fig. 10. Vortex structure in the anisotropic Ginzburg-Landau theory. Geometrical relation between the penetration depth and the coherence length is shown.

$d_{Ag}$ , for which in turn the variation of  $\xi_{GL\parallel}(0)$  should be responsible because  $\lambda_{GL}(0)$  is rather insensitive to  $d_{Ag}$  (see Fig. 9b).

According to Ref. 13,  $\kappa$  for V metal with the mean free path of about 22 Å, which corresponds to the value of 100-Å thick layers in our samples, can be estimated at 10. In Fig. 11b, one finds that multilayering with thin Ag layers raises  $\kappa$  over 10, while with thicker Ag layers  $\kappa$  is lowered below 10.

This result leads us to speculate the possibility of synthesis of type-I superconductors composed of type-II superconductor and normal metal. As seen in Fig. 11, Ag-rich multilayers with rather large  $d$  would be a good candidate. Considering that the V layers in our samples are very dirty, further suppression of  $\kappa$  could be attainable by improving the conditions of sample preparation so that V layer becomes structurally cleaner. In particular, if the condition  $\kappa_{\perp} < 2^{-1/2} < \kappa_{\parallel}$  be satisfied, very interesting material is to be realized, which is type-I in the field perpendicular to the layers, but is type-II in the parallel field.

## VII. CONCLUDING REMARKS

We have investigated the magnetic properties of V/Ag proximity-coupled superconducting multilayers.

First, the electron mean free path in each layer ( $l_V$  and  $l_{Ag}$ ) was extracted from the normal-state resistivity parallel to the layers:  $l_V$  is thickness-dependent up to about 100 Å of V-layer thickness, reflecting the V/Ag boundary scattering, and then reaches the intrinsic value of about 22 Å. In contrast,  $l_{Ag}$  is restricted almost completely by the boundary scattering and is approximated by 1.3 times of the Ag-layer thickness.

Referring to the above transport properties, the layer-thickness dependence of  $\lambda$  was studied. For samples with thin layers,  $\lambda$  decreases with the increase of layer

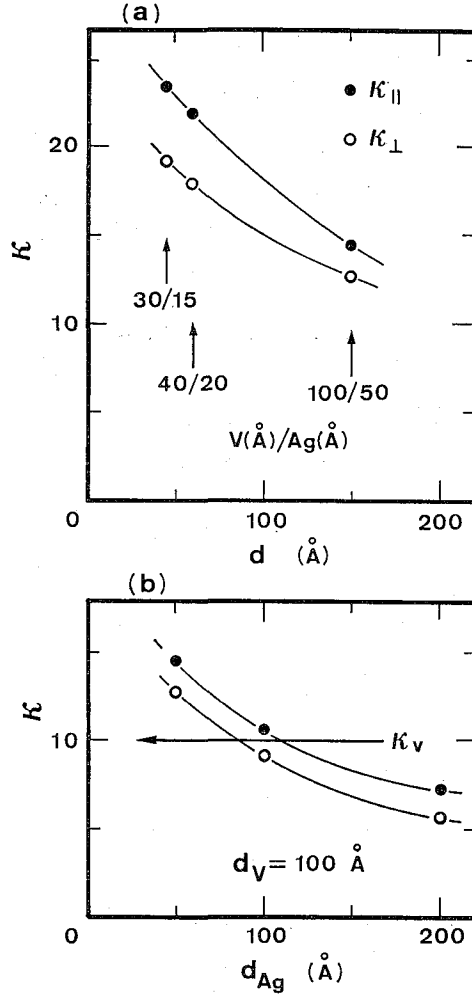


Fig. 11. Parallel and perpendicular Ginzburg-Landau parameters vs multilayer period (a) or Ag-layer thickness (b).  $\kappa_V$  in (b) is for V metal with the mean free path of about 22 Å.

thickness. In this region, the observed behavior is in good agreement with a homogeneous superconductor with the same transition temperature and resistivity. Such a correspondence has been theoretically pointed out only in the thermodynamic properties such as the specific heat.<sup>26)</sup> Our result suggests that this can be generalized to the weak-field electromagnetic properties. When the layer thickness exceeds a critical value, however,  $\lambda$  in turn starts to increase. This feature is considered as a crossover from a single superconductor to a composite one, because the superconducting coupling between the V layers becomes weaker when the Ag layer becomes thicker.

The above situation is also reflected on the temperature dependence of  $\lambda$ . For samples with thin layers,  $\lambda(t)$  is rather similar to a homogeneous superconductor in

the dirty local limit. When the layer thickness increases, however,  $\lambda(t)$  deviates more and more from any limiting behavior of homogeneous superconductors, and exhibits the character of proximity effect.

Next we discussed the Ginzburg-Landau parameter  $\kappa$ . In our system,  $\kappa$  is anisotropic and decreases with an increase of the multilayer period or the Ag layer thickness. The remarkable point is the controllability of  $\kappa$ ; multilayering with thin Ag layers yields  $\kappa$  higher than  $\kappa_V$  in V layer, while with thicker Ag layers,  $\kappa$  becomes smaller than  $\kappa_V$ .

#### ACKNOWLEDGMENTS

Special thanks are due to T. Yamada for his cooperation in sample preparation. This work was supported in part by a grant-in-aid for scientific research from the Ministry of Education, Science, and Culture of Japan.

#### REFERENCES

- (1) S.T. Ruggiero and M.R. Beasley, in *Synthetic Modulated Structures*, ed. by L. Chang and B.C. Giessen (Academic Press, New York, 1985) p. 365.
- (2) P.R. Broussard, D. Mael, and T.H. Geballe, *Phys. Rev. B*, **30**, 4055 (1984).
- (3) S.T. Ruggiero, T.W. Barbee, Jr., and M.R. Beasley, *Phys. Rev. Letters*, **45**, 1299 (1980); *Phys. Rev. B*, **26**, 4894 (1982).
- (4) C.S.L. Chun, G.-G. Zheng, J.L. Vicent, and I.K. Schuller, *Phys. Rev. B*, **29**, 4915 (1984).
- (5) K. Kanoda, H. Mazaki, T. Yamada, N. Hosoito, and T. Shinjo, *Phys. Rev. B*, **33**, 2052 (1986).
- (6) H. Homma, C.S.L. Chun, G.-G. Zheng, and I.K. Schuller, *Phys. Rev. B*, **33**, 3562 (1986).
- (7) H.K. Wong, B.Y. Jin, H.Q. Yang, J.B. Ketterson, and J.E. Hilliard, *J. Low Temp. Phys.*, **63**, 307 (1986).
- (8) K. Kanoda, H. Mazaki, N. Hosoito, and T. Shinjo, *Phys. Rev. B* (to be published).
- (9) K. Kanoda, H. Mazaki, T. Yamada, N. Hosoito, and T. Shinjo, *Phys. Rev. B*, **35**, 415 (1987).
- (10) T. Ishida, K. Kanoda, and H. Mazaki, *Bull. Inst. Chem. Res., Kyoto Univ.*, **61**, 45 (1983); T. Ishida, K. Kanoda, H. Mazaki, and I. Nakada, *Phys. Rev. B*, **29**, 1183 (1984).
- (11) M. Tinkham, *Introduction to Superconductivity* (McGraw-Hill, New York, 1975).
- (12) For multilayers with  $d_{Ag}$  less than 100 Å, the contribution of 100-Å thick outermost Ag layers to the resistivity was subtracted from the raw data.
- (13) C.M. Soukoulis and D.A. Papaconstantopoulos, *Phys. Rev. B*, **26**, 3673 (1982).
- (14) N.W. Ashcroft and N.D. Mermin, *Solid State Physics* (Holt, Rinehart, and Winston, New York, 1976) pp. 5, 757.
- (15) G. Deutscher and P.G. de Gennes, in *Superconductivity*, ed. by R.D. Parks (Dekker, New York, 1969) Vol. II, p. 1005.
- (16) J. Bardeen, L.N. Cooper, and J.R. Schrieffer, *Phys. Rev.*, **108**, 1175 (1957).
- (17) See, for example, the Appendix of T.P. Orlando, E.J. McNiff, Jr., S. Foner, and M.R. Beasley, *Phys. Rev. B*, **19**, 4545 (1979).
- (18) As  $\rho$ , we use the values before subtraction of the contribution of 100-Å thick outermost Ag layers, because these are also responsible for the observed  $\lambda$ .
- (19) R.W. Simon and P.M. Chaikin, *Phys. Rev. B*, **23**, 4463 (1981); *ibid.* **30**, 3750 (1984).
- (20) Y. Oda and H. Nagano, *J. Phys. Soc. Japan*, **44**, 2007 (1978); *Solid State Commun.*, **35**, 631 (1980).
- (21) G. Deutscher, J.P. Hurault, and P.A. van Dalen, *J. Phys. Chem. Solids*, **30**, 509 (1969).
- (22) C. Vallette, *Solid State Commun.*, **9**, 891 (1971).
- (23) G. Deutscher, *Solid State Commun.*, **9**, 895 (1971).
- (24) V.Z. Kresin, *Phys. Rev. B*, **32**, 145 (1985).
- (25) Simon and Chaikin have theoretically studied the spatial profile of magnetic field in proximity-effect bilayer (Ref. 19). Development of such a treatment to the case of multilayers may be useful.
- (26) M.P. Zaitlin, *Phys. Rev. B*, **25**, 5729 (1982); *Solid State Commun.*, **41**, 317 (1982).